



## OPEN

## SUBJECT AREAS:

BIONANO ELECTRONICS  
NANOSCALE BIOPHYSICSReceived  
2 December 2013Accepted  
13 May 2014Published  
30 May 2014

Correspondence and requests for materials should be addressed to N.G. (sunzaghi@seu.edu.cn; guning@seu.edu.cn)

\* These authors contributed equally to this work.

# Magnetic assembly-mediated enhancement of differentiation of mouse bone marrow cells cultured on magnetic colloidal assemblies

Jianfei Sun<sup>1\*</sup>, Xuan Liu<sup>2\*</sup>, Jiqing Huang<sup>2</sup>, Lina Song<sup>1</sup>, Zihao Chen<sup>2</sup>, Haoyu Liu<sup>2</sup>, Yan Li<sup>1</sup>, Yu Zhang<sup>1</sup> & Ning Gu<sup>1</sup>

<sup>1</sup>State Key Laboratory of Bioelectronics, Jiangsu Key Laboratory of Biomaterials and Devices, School of Biological Science and Medical Engineering, Southeast University, Dingjiaqiao 87, Nanjing, P. R. China, 210009, <sup>2</sup>School of Medicine, Southeast University, Dingjiaqiao 87, Nanjing, P. R. China, 210009.

Here we reported an interesting phenomenon that the field-induced assemblies of magnetic nanoparticles can promote the differentiation of primary mouse bone marrow cells into osteoblasts. The reason was thought to lie in the remnant magnetic interaction inside the assemblies which resulted from the magnetic field-directed assembly. Influence of the assemblies on the cells was realized by means of interface effect rather than the internalization effect. We fabricated a stripe-like assemblies array on the glass plate and cultured cells on this surface. We characterized the morphology of assemblies and measured the mechanic property as well as the magnetic property. The cellular differentiation was measured by staining and quantitative PCR. Finally, Fe uptake was excluded as the reason to cause the phenomenon.

Magnetic nanoparticles have attracted increasing interests from biomedical areas, such as hyperthermia<sup>1</sup>, MRI contrast agent<sup>2</sup>, magnetic separation<sup>3</sup> and 3D cell culturing<sup>4</sup>. Recently, receptor-conjugated magnetic nanoparticles can even be used to control the switching of cell death signalling both *in vitro* and *in vivo* by external magnetic field-induced aggregation<sup>5</sup>. All these biomedical applications actually depend upon the biological effects of magnetic nanoparticles. There were numerous publications on the relationship between the colloidal property and the biological effect. Influences of size, shape and surface chemistry of nanoparticles on biological system have been studied<sup>6</sup>. One common feature of nanomaterials is that the collective property depends upon the arrangement of individual units. Thus, the aggregating state should also be an important factor influencing the biological effect of magnetic nanoparticles, just like the case in Ref. 5.

Surprisingly, there are scarce reports on this issue. This is partly because magnetic nanoparticles are often used as “soluble factors” (somewhat like drugs) in many applications. In this case, the nanoparticles are highly stabilized and the distance between two nanoparticles is too far to generate magnetic energy coupling. Therefore, the biological effect caused by the aggregating state can be neglected. However, the arrangement or the alignment of elemental units will play a significant role in some other applications of magnetic nanoparticles, such as polymer/nanoparticles composite scaffold for tissue engineering<sup>7</sup>, cell-ECM (extra-cellular matrix) interaction<sup>8</sup> and implantable devices *in vivo*<sup>9</sup>. These applications mainly utilize the effect of interface between nanoparticles and cells rather than the internalization of nanoparticles into cells. In current reports about these applications, the arrangement of magnetic nanoparticles is commonly random or amorphous. Thus, it is necessary to study the biological effect of interface between the cells and the ordered assemblies of magnetic nanoparticles. The application of magnetic nanoparticles will be deepened and enriched by this research.

On the other hand, the effect of interface between cells and ordered nanoparticulate assemblies is also promising for regulation of cellular behaviour. Currently, the cellular regulation by topography of culturing substrate is increasingly becoming a hot issue because of its great potential in controlling differentiation of stem cells<sup>10–11</sup>. The common method to fabricate micro- or nano-sized surface topography is to use lithography-based techniques. In fact, the assemblies of nanoparticles can have the similar scale with the lithographic-fabricated structures so that the ordered assemblies can also be used to regulate the cellular behaviours. Furthermore, the as-fabricated topographic surface is still the integer of crystal while the assemblies are the aggregates of nanoparticles.

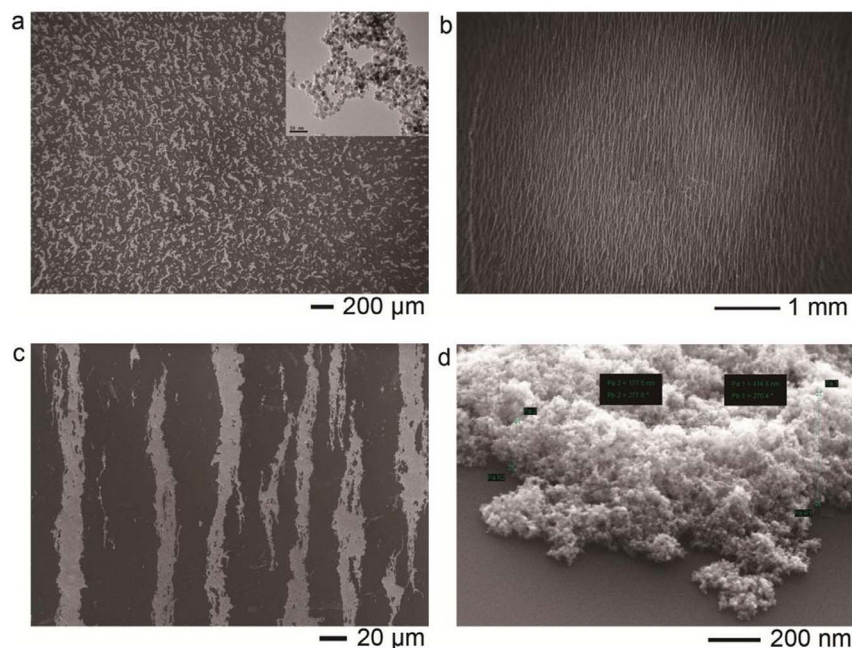


**Figure 1 | Morphology of  $\gamma$ -Fe<sub>2</sub>O<sub>3</sub> nanoparticles.** (a), amorphous aggregates of  $\gamma$ -Fe<sub>2</sub>O<sub>3</sub> nanoparticles after natural drying on Si wafer. Inset: TEM image of synthesized nanoparticles. (b), stripe-like assemblies of  $\gamma$ -Fe<sub>2</sub>O<sub>3</sub> nanoparticles induced by magnetic field on Si wafer. (c), local magnification of (b). (d), the magnified cross-section image of (b).

Considering the similarity of nanoparticles with protein molecules in dimension and property<sup>12–13</sup>, the assemblies of nanoparticles may play a whole new role in the regulation of cellular fate. Especially, the stripe-like assemblies are morphologically somewhat like collagenous fibres, which are the main components of ECM (Extra-Cellular Matrix)<sup>14</sup>. Therefore, we think the stripe-like assemblies of nanoparticles should have an interesting biological effect. For example, it is still a challenging issue whether the coupling of energy between nanoparticles can contribute to the cellular behaviour. Theoretically, due to the very small size, the coupling of energy between nanoparticles will generate a highly local micro-field to significantly influence the close-contacted objects.

In this communication, we fabricated a topographical surface by assembling bare  $\gamma$ -Fe<sub>2</sub>O<sub>3</sub> nanoparticles into stripe-like pattern on glass surface in the presence of an external magnetic field. Then the primary mouse bone marrow cells were cultured on this surface and the differentiation of cells was studied. The bone marrow cells have been reported to have the capability of differentiating into multi-typed cells, including osteoblasts, nerve cells, myocardial cells and so on. In addition, the bone marrow cell-based therapy has been employed to treat many diseases, such as luminal Crohn's disease<sup>15</sup>, cardiac repair<sup>16</sup>, spinal cord injury<sup>17</sup> and autologous bone transplantation<sup>18</sup>. Obviously, the primary bone marrow cell is a good model to study the interface effect of nanoparticulate assemblies both for fundamental research and clinic application. One novelty of our fabricated topological surfaces is that these surfaces have the same topography and elasticity but different magnetic interaction energy. It was discovered that the differential ability of primary bone marrow cells into osteoblasts was influenced by the magnetic coupling inside the assemblies of nanoparticles and the effect was positively dependent upon the field strength of external magnetic field during the assembly process.  $\gamma$ -Fe<sub>2</sub>O<sub>3</sub> nanoparticles were used as building blocks because iron-oxide nanoparticles have been reported to possess protein-like property and capability of promoting bone growth<sup>19–20</sup>. The reason to employ magnetic field-induced assembly is that this method can easily lead to the formation of one-dimensional assemblies in large scale without addition of any other biological or chemical molecules. In our laboratory, we have the ability to assemble

Fe<sub>3</sub>O<sub>4</sub> or  $\gamma$ -Fe<sub>2</sub>O<sub>3</sub> nanoparticles into a parallel stripe-like pattern on substrate in centimetre scale with good order and reproducibility. The surface of  $\gamma$ -Fe<sub>2</sub>O<sub>3</sub> nanoparticles is bare, without any stabilizing agents, which is especially suitable for cell experiments because the inference of stabilizing molecules can be excluded.

## Results

The synthesized super-paramagnetic  $\gamma$ -Fe<sub>2</sub>O<sub>3</sub> nanoparticles were stabilized by surface hydroxylation. The nanoparticles were magnetically separated and washed by ultra-pure water for several times to remove the chemicals in suspension before assembly. Fig. 1a showed the amorphous aggregates of  $\gamma$ -Fe<sub>2</sub>O<sub>3</sub> nanoparticles after natural drying (Inset is the TEM image of as-synthesized nanoparticles). The size distribution, the magnetic property and the  $\zeta$  potential (pH=7) were shown in Supporting Information (Fig. S1). Because there were no stabilizing agents, the nanoparticles formed clusters in suspension. Size of the clusters was about 228 nm so that they can easily be assembled into micro-sized structures in the presence of external magnetic field. The micro-scaled size of the assemblies is beneficial for research of the cellular effect because the size of cell is generally in the micro-scale.  $\zeta$  potential measurement exhibited the surface of nanoparticles was positively charged (+24.3 mV).

To obtain the surface pattern with identical topography with different field strength, the magnetic nanoparticles should have high concentration and be assembled under a uniform magnetic field. Based on the force formula of one magnetic particle under magnetic field ( $F_m = \mu_0 V_p \chi_p \vec{B} \cdot \nabla \vec{B}$ , where  $\mu_0$  is permeability of vacuum,  $V_p$  is volume of magnetic particle,  $\chi_p$  is susceptibility of magnetic particles and  $\vec{B}$  is magnetic flux density, respectively)<sup>21</sup>, the magnetic nanoparticles will not be subjected to the force of a uniform magnetic field. Hence, the attractive force for assembly comes from the magnetic dipolar interaction between the magnetic nanoparticles. Due to the magnetization, the magnetic nanoparticles can be regarded as the magnetic dipoles, which moments are dependent upon the magnetization. If the dipoles are aligned unanimously in the presence of a magnetic field, the force of dipole-dipole interaction between two particles can be described as  $F_m = 6(\vec{m}^2/d^4)$ , where  $\vec{m}$  is magnetic



moment of a magnetic particle and  $d$  is distance between two adjacent particles<sup>22</sup>. Thus, the assembled morphology was mainly determined by the magnetization of particles (particles here were actually the clusters of nanoparticles) and the concentration. Concentration is independent upon the external field and high concentration can guarantee  $d$  is small enough to generate dipolar interaction.  $\vec{m}$  will always keep constant under any external magnetic fields after the particles are magnetized into saturation. Therefore, the increase of field strength will have little influence on the assembled morphology.

Based on the configuration of our field generator, middle area of the field should be uniform because the size of cross-section is two folds over that of the gap. This can be seen from the simulation of field distribution (Supporting Information, Fig. S2). The field strength was set at four values: 20 mT, 40 mT, 80 mT and 120 mT. Based on the magnetization curve, our magnetic nanoparticles have been magnetized to saturation under 10 mT field strength which was far below the minimal strength of magnetic field in our experiments. The colloidal concentration of every experimental sample was 0.1 mg/ml. The morphological characterization by SEM confirmed the above-mentioned analysis that the assembled patterns showed little difference among the samples under different field strength. A typical assembled pattern was shown in Fig. 1b and the local magnification was shown in Fig. 1c and d. It was seen that the stripe-like assemblies were approximately 20  $\mu\text{m}$  wide and about 400 nm high. Interestingly, the assemblies showed better size distribution although the nanoparticles were polydispersed. The stripes were uniformly arranged on the whole surface in parallel with relatively high density. However, the stripes were not straight and continuous, which mainly resulted from the deformation induced by solvent evaporation. We took a video recording the process of deformation (data not shown in this paper). The stripes were formed in the solution straightly and uniformly but they were deformed when the water evaporated to dryness thoroughly.

Before the cell experiments, we also measured the elastic moduli and the hardness of the stripe-like assemblies on Si wafer because the influence of mechanic property of substrate on cellular fate has been extensively reported<sup>23–24</sup>. The measurement was carried out by nanoindenter on three different positions and the average value was calculated by the machine automatically. The results exhibited that the elastic moduli as well as the hardness of different samples, including the naturally-dried aggregates and the stripe-like assemblies induced by magnetic field of different strength were nearly identical (Fig. 2a). Here, the thickness of nanoparticulate layer plays a dominant role. Because the thickness of nanoparticulate layer was just several hundreds of nanometers, the mechanic property measured by the machine as well as sensed by cells will mainly be that of the substrate<sup>25</sup>. In our experiments, it is the Si wafer. Actually, the

standard elastic modulus of Si wafer with oxide layer is 140 GPa. Thus, the different influence on cells should not be attributed to the mechanic property of substrates. Besides, another phenomenon can partly confirm the independence of the cellular effect upon the surface topography. In addition to the bone marrow cell, NK (Natural Killer) cell and DC (Dendritic Cell) cell were also cultured on the assemblies. The difference between bone marrow cell and DC cell or NK cell is that the former is anchorage-dependent cell while the latter is non-adherent cell. During the process of culturing, the DC cells or the NK cells will not adhere to the assemblies but will adsorb on the assemblies like gas bubbles. Thus, the surface topography should hardly influence the non-adherent cells. Nevertheless, we discovered the DC cells or the NK cells were truly influenced by the assemblies (the immunological function was enhanced) and the influence was relative with the field strength in assembly process. Therefore, it was thought that the influence should arise from other factors rather than the surface topography.

Although the morphology of colloidal assemblies showed little variety with increase of the field strength during the assembly process, the energy inside the assemblies was different. In the presence of magnetic field, the energy of magnetic dipole can be written as  $E = -\vec{m} \cdot \vec{B}$ , where  $\vec{m}$  is magnetic moment of dipole and  $\vec{B}$  is magnetic flux density. As above mentioned,  $\vec{m}$  is same for every sample after magnetization into saturation. The assemblies of nanoparticles can be regarded as one total dipole which was comprised of numerous particulate dipoles due to the magnetic coupling. Thus, the total magnetic energy of assemblies is reduced with the increase of external field strength. This also means the structure assembled under the high magnetic field is more stable than that assembled under the low field. During the process of magnetic-directed assembly, the magnetic moments of nanoparticles were also aligned unanimously. After the external magnetic field was removed, thermal fluctuation will make the moments of magnetic nanoparticles into disordered state again. If there is no magnetic dipolar coupling, the magnetic moments of nanoparticles should restore to the totally disordered state and the magnetic moments with counteract with each other. This means the assemblies will exhibit no net magnetic moments. Since that the surfaces of magnetic nanoparticles were bare and contacted closely, the magnetic moments were incapable of restoring to the disordered state thoroughly due to the magnetic dipolar interaction and the surface pinning effect<sup>26–27</sup>. These remnant magnetic moments caused emergence of so-called remanence. Obviously, the assembled structure with higher stability will have the stronger remanence because the assemblies of higher stability have the stronger capability of resisting this magnetic reversal. We used FMR (FerroMagnetic Resonance) to prove this point because

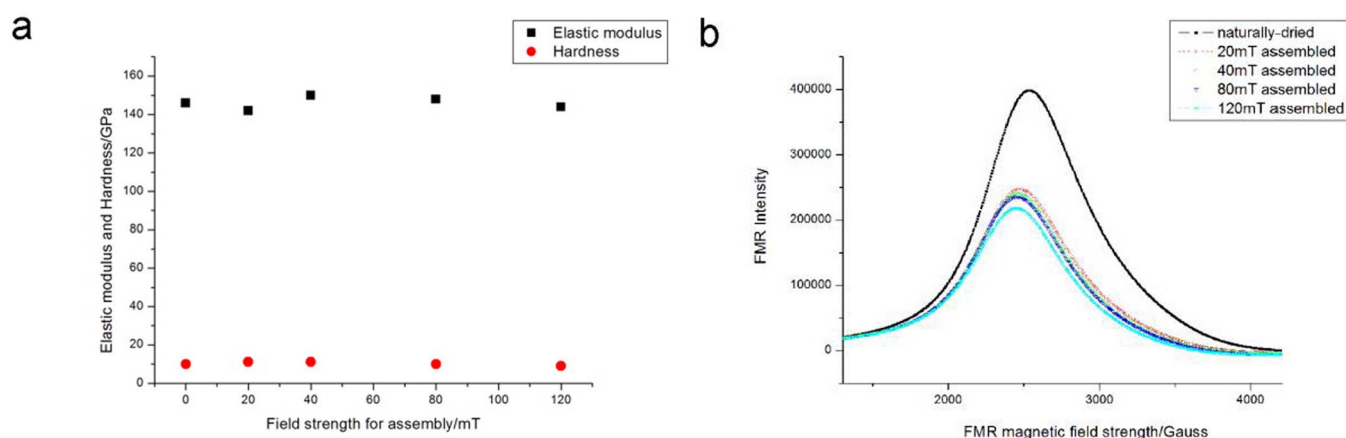


**Figure 2** | characterization of mechanic and magnetic property of Glass/assemblies surface. (a), elastic moduli measured by nanoindenter. (b), FMR spectra.



narrowing of FMR peak indicates magnetic dipolar interaction inside sample<sup>28</sup>. The FMR curves of different samples were shown in Fig. 2b (the magnetic field of FMR measurement was perpendicular to the assemblies). It was exhibited that the resonance peak of assembled samples was much smaller than that of the natural-dried sample and the narrowing of FMR peaks was negatively dependent upon the field strength of assembly. This case demonstrated that there was the strong remnant dipolar interaction inside the assemblies after the field-directed assembly of nanoparticles. To verify the emergence of remanence, the magnetic hysteresis curve of the colloidal assemblies was measured by VSM (Vibrating Sample Magnetometer). The magnetic nanoparticles were assembled in a polyacrylamide solution to get high volume of magnetic nanoparticles. With the process of assembly, the solution gradually translated into the hydrogel and the colloidal assemblies were fixed inside. Then the hydrogel was sent for measurement. The magnetic hysteresis curves of four samples were measured, which were the natural aggregates, the assemblies under 20 mT, 40 mT and 80 mT, respectively (Supporting Information, Fig. S3). Due to the heating of electromagnet, the hydrogel formed under 120 mT field was too bad to get the magnetic hysteresis curve). Seen from the curves, there is an obvious transition that the contour area of hysteresis curve becomes larger, which means the collective magnetic property of nanoparticles turns from super-paramagnetism into ferromagnetism. The intercept of y axis indicates the magnitude of remanence. An important fact here is that the magnetic coupling is anisotropic. Along the parallel direction, the magnetic interaction is significantly enhanced with the increase of field intensity during the assembly process while the tendency along the perpendicular direction is unobvious. This anisotropy is accordant with the direction of magnetic field in assembly.

The emergence of remanence is very important for the interface effect between the assemblies and the close-contacted cells. Here, one stripe of assemblies can be considered as a small magnet. The remanence will generate a gradient magnetic field at the defects of the stripes (such as discontinuity). Because the size of defects was very small, the magnetic force produced by the gradient field can be high enough to influence the micro-environment of cells. This mechanism has been reported to get used to assemble multi-segmented nanowires<sup>29</sup>. Here, the bare surface of nanoparticles is a vital factor for the emergence of remanence because the bare surface can generate strongest dipolar coupling. If the magnetic nanoparticles were capped by a thick stabilizing layer, the energy coupling between nanoparticles will be too weak to overcome the thermal fluctuation. In this case, the magnetic moments will thoroughly restore to the disordered state when the external field was removed. We also measured the FMR spectrum of DMSA-capped  $\gamma$ -Fe<sub>2</sub>O<sub>3</sub> nanoparticles which was proved to have the thicker capping layer and the high stability in solution<sup>30</sup>. The result showed that the FMR spectra of the naturally-dried sample and the field-assembled sample had little difference (Supporting Information, Fig. S4).

With the assembly by magnetic field, the magnetic nanoparticles can be assembled well on several substrates including silicon, glass and plasma-treated PLA. We had carried out some preliminary experiments on these substrates with 3T3 cell line. It was observed that the cells showed a nearly same behaviour in spite of culturing on different substrates. Therefore, it was thought the cellular behaviour should be mainly affected by the assemblies of nanoparticles rather than the substrates. Then the primary mouse bone marrow cells were cultured on the glass/assemblies surfaces for ease of observation. The cellular viability was measured by a flow cytometry and the cells on three plates were collected for measurement. The result showed that the glass/assemblies surface was well biocompatible for the cells and the presence of  $\gamma$ -Fe<sub>2</sub>O<sub>3</sub> nanoparticles can even promote the viability of bone marrow cells on glass substrate (Supporting Information, Fig. S5). It was seen that the natural-aggregates of nanoparticles on glass showed the worst biocompatibility. The cellular viability was

only 67.03%, even below that of bare glass, which was 77.15%. However, the stripe-like assemblies showed a much better biocompatibility. The minimal viability was 86.09% and the maximal viability can reach 96.85%, better than that of the natural aggregates about 1.44 folds. This difference can be explained by the case that the assemblies can play a role of the sites for cell adhesion. In our preliminary experiments, it was observed that the cells preferred to adhere to the stripe-like assemblies of  $\gamma$ -Fe<sub>2</sub>O<sub>3</sub> nanoparticles (Supporting Information, Fig. S6). The same phenomenon was not observed for the natural aggregates.

The optical image of cellular colony formation on the stripe-like assemblies (under 20 mT field strength) after 6 days culturing was shown in Fig. 3a, seen from which the cells spread out well and aggregated together closely. This means the cells start to differentiate. Here it should be mentioned that the inducing agents were also added during the cell culturing. Actually the cells were induced to differentiate by association of inducing agents and the assemblies. Then the differentiation of primary bone marrow cells were measured by ALP (Alkaline Phosphatase) staining. ALP is a common indicator of differentiation into osteoblast. The area and the thickness of colour denote the degree of cellular differentiation. Here the commercial culturing plate and the bare glass plate were used as control. The staining patterns were shown in Fig. 3b and western blotting technique was also used for confirmation (Supporting Information, Fig. S7). The results from these two techniques matched well. The thickness of western blotting bands exhibited the same tendency as the result of staining. An interesting phenomenon was that the cells culturing on the stripe-like assemblies exhibited more differentiation than those culturing on the amorphous aggregates of  $\gamma$ -Fe<sub>2</sub>O<sub>3</sub> nanoparticles. Moreover, the assemblies induced by the higher field have stronger capability of enhancing the differentiation of bone marrow cells. This phenomenon was reproducible and we measured the mRNA expression of osteocalcin and ALP by quantitative PCR to further confirm the result on protein level (All q-PCR original files can be find in Supplementary Materials). Here, osteocalcin, same as ALP, is also a specific biomarker for osteoblasts differentiation and maturation. The q-PCR results were shown in Fig. 3c, which also exhibited the promotion of cellular differentiation and the dependence upon the field strength of assembly. The linear correlation coefficients between the width of FMR peak and the values of q-PCR were calculated. The width of FMR was defined as the peak width at half height and all the FMR peaks were normalized. Here it should be mentioned that the width of FMR peak can reflect the magnetic coupling but it is not the direct quantitative indicator of the magnetic interaction. The linear correlation coefficient between the width of FMR peak and the ALP expression was 0.60168 while the linear correlation coefficient between the width of FMR peak and the osteocalcin expression was 0.66545. This result explained that the enhancement of differentiation to osteoblasts is truly correlative with the magnetic coupling between magnetic nanoparticles. Also, it seemed the magnetic effect of colloidal assemblies on osteocalcin is more than that on ALP. The increments of q-PCR value for four samples of assemblies were 0.28799, 2.3975 and 1.00732, respectively. The ratios of increase were 1.8 folds, 5.4 folds and 0.35 fold, respectively. Therefore, although the mRNA expression value of assemblies sample under 120 mT was highest, the maximal increment of mRNA expression value was caused by the assemblies sample under 80 mT.

To preliminarily study the signal pathway, the mRNA expression as well as the protein expression of BMP-2 (Bone Formation Protein) and *Runx2* were also measured by quantitative PCR and western blotting, respectively. BMP-2 is an important regulation protein to induce the differentiation of osteoblasts and enhance the formation of bone. *Runx2* is a critical transcription factor for osteoblasts formation and *Runx2* is the downstream of BMP-2. The q-PCR and the western blotting results also exhibited a positive dependence upon

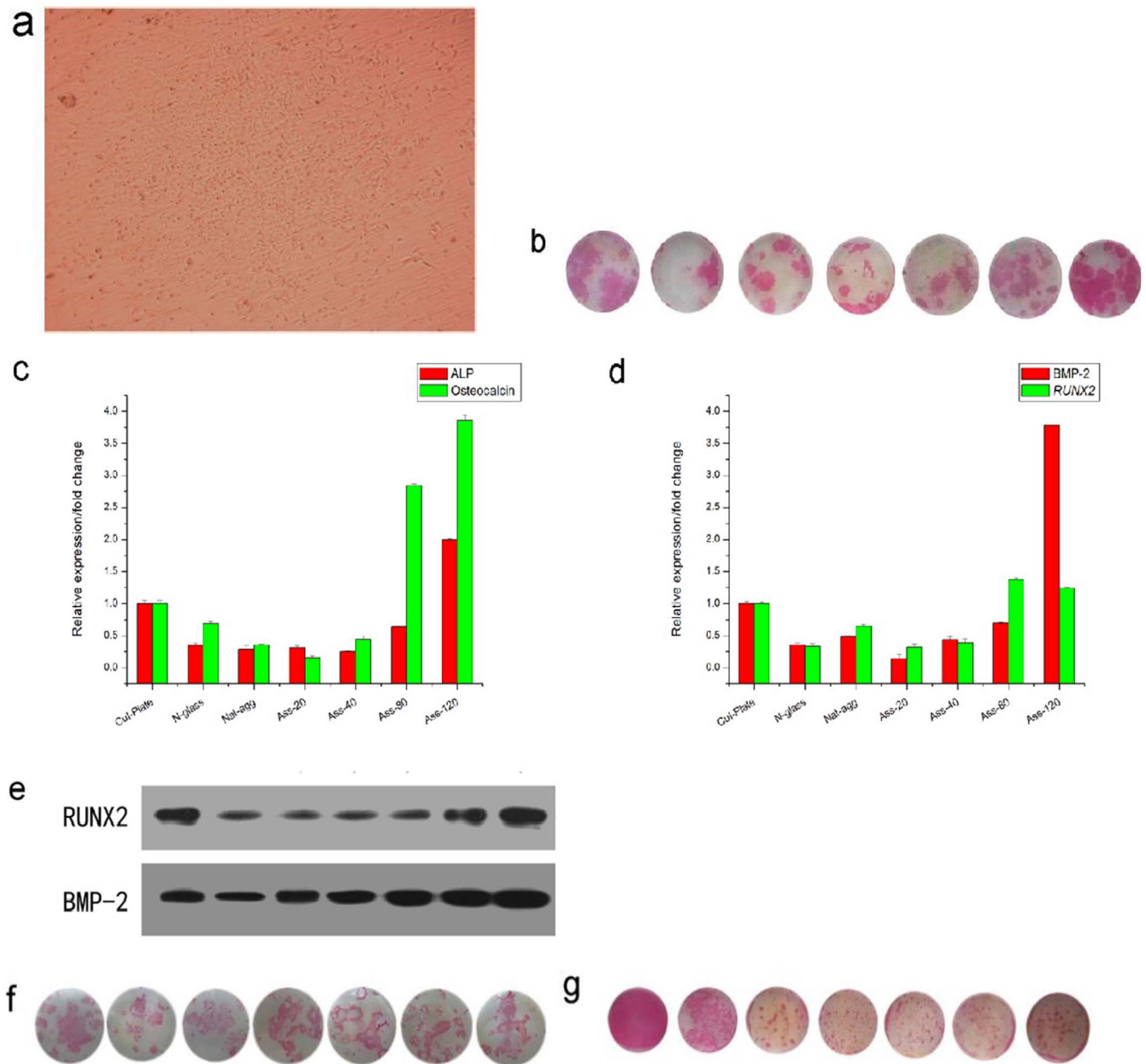


**Figure 3 | Differentiation of primary mouse bone marrow cells.** (a), optical observation of colony formation of cells cultured on the assemblies. Magnification:  $\times 5$ . (b), ALP staining of cells cultured on the different substrates. From the left to the right: commercial culturing plate, bare glass plate, the naturally-dried aggregates, the stripe-like assemblies fabricated by 20 mT field, the stripe-like assemblies fabricated by 40 mT field, the stripe-like assemblies fabricated by 80 mT field, the stripe-like assemblies fabricated by 120 mT field. (c) and (d), mRNA expression of ALP/Osteocalcin and BMP-2/RUNX2 of cells on different substrates, respectively. Here Cur-plate means the commercial culturing plate for cells. N-glass means the bare glass plate. Nat-agg means the naturally-dried aggregates of nanoparticles. Ass-20, Ass-40, Ass-80 and Ass-120 mean the stripe-like assemblies fabricated under the 20 mT, 40 mT, 80 mT and 120 mT field strength, respectively.  $*p < 0.05$  (calculated between two samples) (e), Western Blotting measurement of ALP expression. From the left to the right: commercial culturing plate, bare glass plate, the naturally-dried aggregates, the stripe-like assemblies fabricated by 20 mT field, the stripe-like assemblies fabricated by 40 mT field, the stripe-like assemblies fabricated by 80 mT field, the stripe-like assemblies fabricated by 120 mT field. (f), ALP staining of cells cultured on the different substrates after thermal treatment for over 8 hours. From the left to the right: commercial culturing plate, bare glass plate, the naturally-dried aggregates, the stripe-like assemblies fabricated by 20 mT field, the stripe-like assemblies fabricated by 40 mT field, the stripe-like assemblies fabricated by 80 mT field, the stripe-like assemblies fabricated by 120 mT field. (g), ALP staining of cells cultured on the different substrates in the presence of magnetic field. From the left to the right: commercial culturing plate, bare glass plate, the naturally-dried aggregates, the stripe-like assemblies fabricated by 20 mT field, the stripe-like assemblies fabricated by 40 mT field, the stripe-like assemblies fabricated by 80 mT field, the stripe-like assemblies fabricated by 120 mT field.

the field strength of assembly (Fig. 3d, e). Therefore, it was supposed that the increased expression of BMP-2 caused the up-regulation of *Runx2* which resulted in the enhancement of cellular differentiation. Likewise, the linear correlative coefficients between the magnetic

coupling and expression of BMP-2 and *Runx2* were also calculated. The results were 0.54053 and 0.43417, respectively. It was showed the magnetic effect of colloidal assemblies can affect the signal pathway. However, the correlation seemed not to be so strong. This may be due



to the complex cascaded signal pathways of cellular differentiation toward osteoblasts. BMP2-Runx2 is just one common signal pathway but the local micro-magnetic field from the assemblies of magnetic nanoparticles may affect the bone marrow cells via other known or unknown pathways. It has been beyond the category of this paper to well define the molecular mechanism. Here, the cells were thought to be affected by the local micro-magnetic field from the assemblies of magnetic nanoparticles. The cells were actually subjected to two effects. One was the assemblies of nanoparticles. The other was the local magnetic field. Hence, the real mechanism may be totally novel and very complex. For example, we observed that the cytoskeleton of some cells was elongated and re-arranged to the edge by the assemblies (Supporting Information, Figure S8). It will be our next goal to discover the real molecular mechanism of colloidal assemblies – mediated magnetic effect on primary bone marrow cells.

## Discussion

As the above mentioned analysis, the remanence here was considered to play an important role. Here, the remanence makes the assemblies somewhat like micro magnets. Then the cells will be subjected to the highly local magnetic field. It has been reported that the presence of external field, such as electric field, static magnetic field and extremely low-frequency electromagnetic field can influence the differentiation of stem cells<sup>31–33</sup>. We thought there may be a similar mechanism here. It is the local magnetic field arising from the colloidal assemblies to affect the cells.

Because the magnetic field induced by the remanence is highly localized, it is hard to measure the influence of this field directly. However, we can indirectly prove the role of the magnetization of assemblies in the cellular differentiation. Firstly, if the hypothesis is right, the effect of colloidal assemblies on the cells should be identical with that of the natural aggregates provided that the assemblies of magnetic nanoparticles are all de-magnetized. Demagnetization means the influence of remanence is excluded. It is well known that high temperature can demagnetize magnetic materials. Therefore, the samples, including the assemblies and the natural aggregates were treated under 120°C for over 8 hours. This temperature will not change the assembled morphology of  $\gamma$ -Fe<sub>2</sub>O<sub>3</sub> nanoparticles. Then the primary mouse bone marrow cells were cultured on these surfaces. The ALP staining results confirmed our supposition (See Fig. 3f). After the treatment of demagnetization, the assemblies under different field intensities showed the nearly same influence as that of the natural aggregates on the cells, which partly verified the above-observed phenomenon resulted from the effect of remanence. On the other hand, the cellular differentiation will also become identical if the magnetization of nanoparticulate assemblies was same. This means the difference of magnetic dipolar interactions is neglected. This point can be realized by culturing the primary mouse bone marrow cells in the presence of a strong external magnetic field perpendicular to the assemblies. In this case, the assemblies will be magnetized along the perpendicular direction. Because the external magnetic field is much stronger than the remanence, the influence of the remanence on the magnetization can be neglected. In our experiments, the magnetic field was generated by a cylindrical permanent magnet and perpendicular to the glass plate. The magnetic field was actually distributed with gradient and the strength at cell position was about 150 mT. The ALP staining result was shown in Fig. 3g, seen from which the magnetostatic field promoted the differentiation of cells culturing on the commercial cell plate as well as on the bare glass plate but the differentiation of cells culturing on the  $\gamma$ -Fe<sub>2</sub>O<sub>3</sub> nanoparticles was prohibited, including the amorphous aggregates and the stripe-like assemblies. For the amorphous aggregates and the stripe-like assemblies of  $\gamma$ -Fe<sub>2</sub>O<sub>3</sub> nanoparticles, the staining pattern was the discrete dots and exhibited little difference among the samples. The result can prove the above-proposed hypothesis. Firstly, the magnetic field seemed conducive to the differentiation of primary

mouse bone marrow cells, which can explain the promotion of remanence to the cellular differentiation. Secondly, the assimilation of staining patterns for cells culturing on different assembled samples indicated that the cellular differentiation was indeed regulated by the magnetization of the assemblies. If the assemblies fabricated under the different field strength were magnetized into the same state, the influence of different assemblies on cellular differentiation was also same. About this point, we will make an analysis in detail as the following.

In the presence of a strong external magnetostatic field, the cells were mainly influenced by effect of the external field rather than the remanence. However, the magnetic nanoparticles layer, including the amorphous aggregates and the stripe-like assemblies, can modulate the external magnetic field. For the cells culturing on the surface of glass/ $\gamma$ -Fe<sub>2</sub>O<sub>3</sub> nanoparticles, the layer of magnetic nanoparticles actually played a ‘shielding’ role. For the closely-contacted magnetic nanoparticles, the assemblies can be regarded as the continuous magnetic medium. When the continuous magnetic medium was magnetized under the perpendicular magnetic field, the magnetic flux was restricted into the medium rather than dissipated in the free space. The field distribution of three cases, including the remanence at the gap of assemblies, the perpendicular external field in the absence of the colloidal assemblies and the perpendicular external field at the gap of assemblies were schematically shown in Fig. 4 where the assemblies of nanoparticles were regarded as the continuous magnetic medium. Obviously, the field strength on cells was weakened due to the restriction of magnetic flux. Only at the discontinuous positions of magnetic aggregates or assemblies, there was the drained magnetic field that can influence the cellular differentiation nearby. Thus, the staining pattern for cells culturing on aggregates and assemblies was the discrete dots. For stripe-like assemblies of magnetic nanoparticles induced by the different field strength, the modulation of external field was same due to the identical morphology so that the staining patterns for different samples exhibited no difference. From this experiment, the dependence of cellular differentiation upon the magnetic energy was confirmed.

Finally, we did prussian blue staining to check whether the influence came from the Fe uptake. The result was shown in Supporting Information (Fig. S9). Seen from the images, the cells cultured on the aggregated nanoparticles exhibited very tiny Fe uptake compared with those cultured on the bare glass plate and the commercial culturing plate. Interestingly, the Fe uptake of cells cultured on the stripe-like assemblies was even less than that of cells cultured on the naturally-dried aggregates, which may result from the higher stability of the assemblies. We also utilized q-PCR to measure the mRNA expression of lactoferrin for quantitatively study the nanoparticle uptake because lactoferrin can be over-expressed to regulate the Fe ions if there are extra-Fe coming into cells. The result was shown in Supporting Information (Fig. S10), seen from which the cells cultured on the assemblies had the less Fe uptake than those cultured on the aggregates. Actually, the assembled nanoparticles were also noticed to be more stable in our daily experimental operations. Anyway, the difference of cellular differentiation is not caused by the nanoparticles uptake.

We also did Von Kossa staining to observe the formation of calcium nodules after culturing the cells for over 30days. This experiment is to check the osteogenesis capability of the primary cells. However, although the magnetic nanoparticles can enhance the differentiation of primary bone marrow cells, the osteogenesis result was not good. The poor capability of long-term culturing of cells can account for this case. The substrate of colloidal assemblies is bare glass without modification of any biologically-active components. It has been known the bare glass is not a good biomaterial *in vivo*. Also, just as our data in cellular viability experiment, bare surface of glass is not well biocompatible, especially for primary cells. In our laboratory, it was observed there were many cells shed from the substrate

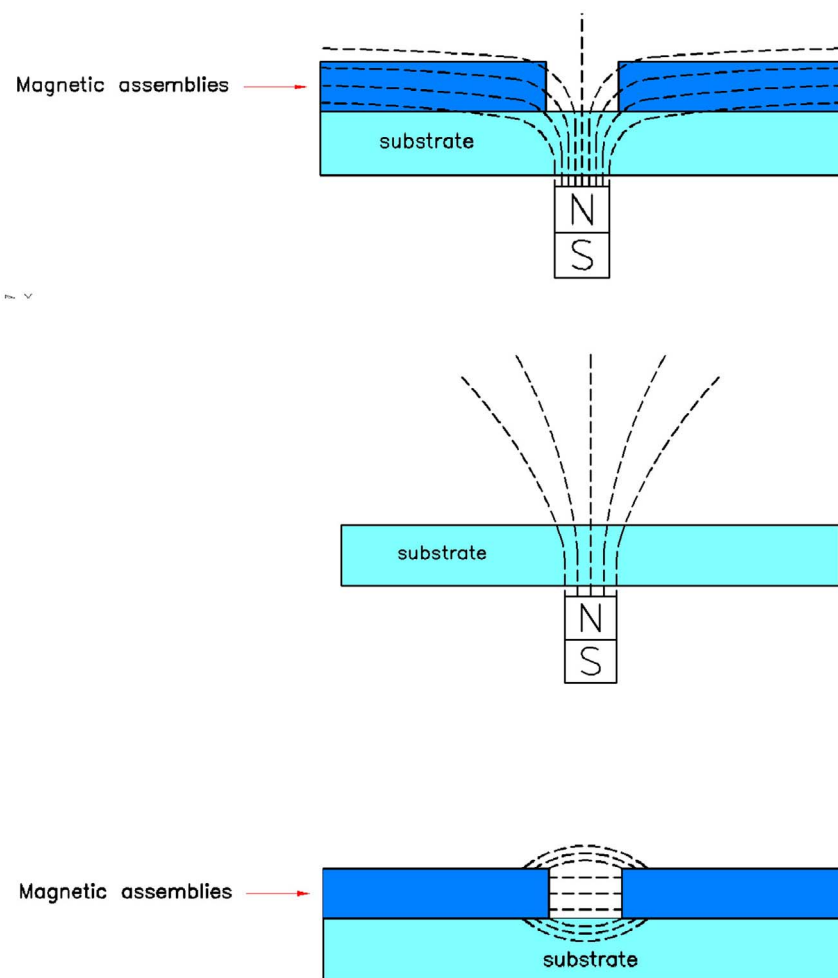


**Figure 4** | Schematic show of three cases of field distribution in our experiments. (a), the restriction of magnetic flux at the gap of magnetic assemblies in the presence of the perpendicular external magnetic field. (b), the magnetic flux without magnetic assemblies in the presence of the perpendicular external magnetic field. (c), the remanence-induced magnetic flux at the gap of stripe-like assemblies in the absence of the external magnetic field.

after 20 days culturing. Thus, the osteogenesis was prohibited. To take advantage of magnetic nanoparticles in clinic bone repair, it must be noticed that the nanoparticles should be integrated with well-biocompatible materials and can keep cells long-term culturing.

In conclusion, a novel phenomenon was discovered that the magnetic energy inside the assemblies of magnetic nanoparticles can enhance the differentiation of primary mouse bone marrow cells culturing on the assemblies into osteoblasts. The mechanism may lie in the influence on cells of high gradient magnetic field which arose from the remnant magnetic interaction inside the assemblies at the positions of continuity broken. The emergence of remnant magnetic interaction inside assemblies was the specific feature of magnetic field-directed assembly of nanoparticles because only this assembly can lead to the unanimous alignment of magnetic moments accompanied with the formation of stripes. Due to the different stability of assembled structures, the relaxation (restore the disordered state) of magnetic moments was also different after the external field was removed. With the increasing interests in research of cellular regulation, such as the controlled differentiation of stem cells and induced pluripotent stem cells, the biophysical factors besides cytokine, get more and more attentions. Our results about the cellular regulation with nanoparticles-mediated magnetic effect will be favourable for the intensive investigation and extensive application of stem cell technology.

## Methods

**Synthesis of bare  $\gamma$ -Fe<sub>2</sub>O<sub>3</sub> nanoparticles:** the 25% (w/w) N(CH<sub>3</sub>)<sub>4</sub>OH was slowly added into the mixture of Fe<sup>2+</sup> and Fe<sup>3+</sup> (molar ratio is 1:2) until the pH reached 13. Then the reaction continued for 1 h to obtain the black colloidal particles (Fe<sub>3</sub>O<sub>4</sub>). Then the air was pumped into the reaction system under the 95 °C water bathing after the pH was adjusted to 3. Finally, the reaction system was kept for 3 h to oxidize Fe<sub>3</sub>O<sub>4</sub> colloidal particles into  $\gamma$ -Fe<sub>2</sub>O<sub>3</sub> nanoparticles. During the whole reaction, the vigorous stirring was needed.

**Assembly of nanoparticles:** the synthesized nanoparticles were purified by centrifugal separation and magnetic separation for several times until pH=7. Then a drop of 60  $\mu$ l colloidal suspension was put on the substrate. For SEM characterization, the substrate was Si wafer (1 cm  $\times$  1 cm) and for cellular experiments, the substrate was the rounded glass plate. Both the two substrate were cleaned by the boiling mixture of H<sub>2</sub>O<sub>2</sub>/H<sub>2</sub>SO<sub>4</sub> (volume ratio: 1:3). The magnetic field was generated by a C-shaped solenoid and the field strength can be changed by tuning the excitation current. The cross-section was 4  $\times$  4 cm<sup>2</sup> and the gap was 2 cm. The Si wafer or the glass plate was on the middle of the gap so that the field was uniform at this position. During the assembly, the field was parallel to the substrate and was present until the colloidal suspension was dried thoroughly.

**Mouse bone marrow cell extraction:** several C57/B6 mice were killed and were dipped in 70% ethanol for tens of seconds. Then the femur and tibia were cut and put in 5 ml  $\alpha$ -MEM medium. The skin and muscle were removed and the both ends of bones were cut down. A 25G needle was used to flush the bone marrow out into the  $\alpha$ -MEM medium. Then the medium containing the bone marrow was transferred to a 15 ml tube for centrifugal separation with 2000rpm for 5 min. the pellets were resuspended in the cell culture medium ( $\alpha$ -MEM with 15% FBS and 1% Penicillin-Streptomycin) after aspirating the supernatant. Before the culturing, the cells were counted and adjusted to a suitable concentration for cell seeding. The detailed operation can refer to Ref. 34. This experiment was performed in accordance with the relevant regulations and the experimental qualification was approved by Southeast



University and Chinese government (Department of Science and Technology of Jiangsu province).

Culturing of primary mouse bone marrow cells: the extracted bone marrow cells were cultured in 24-well plate with 3 wells as one group. The size of one well is just 1.5 cm so that the rounded glass plate with assemblies of nanoparticles can be just put into the well. The culturing medium was the  $\alpha$ -MEM medium containing 15% fetal bovine serum and 1% Penicillin-Streptomycin. The ascorbic acid-2-phosphate (1 mM) was added into the culturing medium to initiate differentiation. The culturing medium was changed every 3 days. After culturing for about 10 days, multicellular fibroblastoid colonies (or CFU-fs) can be observed. These colonies were stained to check expression of alkaline phosphatase by using a reagent kit (bought from Sigma Co.).

- Sharifi, I., Shokrollahi, H. & Amiri, S. Ferrite-based magnetic nanofluids used in hyperthermia applications. *J. Mag. Mag. Mater.* **324**, 903–915 (2012).
- Lee, N. & Hyeon, Y. Design synthesis of uniformly sized iron oxide nanoparticles for efficient magnetic resonance imaging contrast agents. *Chem. Soc. Rev.* **41**, 2575–2589 (2012).
- Pan, Y., Du, X., Fan Zhao, & Bing Xu, Magnetic nanoparticles for the manipulation of proteins and cells. *Chem. Soc. Rev.* **41**, 2912–2942 (2012).
- Rocha, E. L., Porto, L. M. & Rambo, C. R. Nanotechnology meets 3D in vitro models: Tissue engineered tumors and cancer therapies. *Mater. Sci. Eng. C* **34**, 270–279 (2014).
- Cho, M. H. *et al.* A magnetic switch for the control of cell death signalling in vitro and in vivo systems. *Nat. Mater.* **11**, 1038–1043 (2012).
- Albanese, A., Tang, P. S. & Chan, W. C. W. The effect of nanoparticle size, shape, and surface chemistry on biological systems. *Annu. Rev. Biomed. Eng.* **14**, 1–16 (2012).
- Shi, J., Votruba, A. R., Farokhzad, O. C. & Langer, R. Nanotechnology in drug delivery and tissue engineering: From discovery to applications. *Nano Lett.* **10**, 3223–3230 (2010).
- Mendes, P. M. Cellular nanotechnology: making biological interfaces smarter. *Chem. Soc. Rev.* **42**, 9207–9218 (2013).
- Vaddiraju, S., Tomazos, I., Burgess, D. J., Jain, F. C. & Papadimitrakopoulos, F. Emerging synergy between nanotechnology and implantable biosensors: A review. *Biosens. Bioelectron.* **25**, 1553–1565 (2010).
- Lord, M. S., Foss, M. & Besenbacher, F. Influence of nanoscale surface topography on protein adsorption and cellular response. *Nano Today* **5**, 66–78 (2010).
- Hoffman-Kim, D., Mitchel, J. A. & Bellamkonda, R. V. Topography, cell response, and nerve regeneration. *Annu. Rev. Biomed. Eng.* **12**, 203–231 (2010).
- Pelaz, B. *et al.* The State of Nanoparticle-Based Nanoscience and Biotechnology: Progress, Promises, and Challenges. *ACS Nano* **6**, 8468–8483 (2012).
- Kotov, N. A. Inorganic nanoparticles as protein mimics. *Science* **330**, 188–188 (2010).
- Parenteau-Bareil, R., Gauvin, R. & Berthod, F. Collagen-based biomaterials for tissue engineering applications. *Materials* **3**, 1863–1887 (2010).
- Duijvestein, M. *et al.* Autologous bone marrow-derived mesenchymal stromal cell treatment for refractory luminal Crohn's disease: results of a phase I study. *Gut* **59**, 1662–1669 (2010).
- Loffredo, F. S., Steinhauser, M. L., Gannon, J. & Lee, R. T. Bone Marrow-Derived Cell Therapy Stimulates Endogenous Cardiomyocyte Progenitors and Promotes Cardiac Repair. *Cell Stem Cell* **8**, 389–398 (2011).
- Wright, K. T., Masri, W. E., Osman, A., Chowdhury, J. & Johnson, W. E. B. Concise Review: Bone Marrow for the Treatment of Spinal Cord Injury: Mechanisms and Clinical Applications. *Stem Cells* **29**, 169–178 (2011).
- Chanda, D., Kumar, S. & Ponnazhagan, S. Therapeutic potential of adult bone marrow-derived mesenchymal stem cells in diseases of the skeleton. *J. Cell Biochem.* **111**, 249–257 (2010).
- Lizeng Gao, *et al.* Intrinsic peroxidase-like activity of ferromagnetic nanoparticles. *Nat. Nanotechnol.* **2**, 577–583, (2007).
- Jie Meng, *et al.* Super-paramagnetic responsive nanofibrous scaffolds under static magnetic field enhance osteogenesis for bone repair *in vivo*. *Sci. Rep.* **3**, 2655–2661 (2013).
- Friedman, G. & Yellen, B. Magnetic separation, manipulation and assembly of solid phase in fluids. *Curr. Opin. Colloid & Interf. Sci.* **10**, 158–166 (2005).
- Ge, J. P., Hu, Y. X., Zhang, T. R., Huynh, T. & Yin, Y. D. Self-assembly and field-responsive optical diffractions of superparamagnetic colloids. *Langmuir* **24**, 3671–3680 (2008).
- Guilak, F. *et al.* Control of Stem Cell Fate by Physical Interactions with the Extracellular Matrix. *Cell Stem Cell* **5**, 17–26 (2009).
- Voge, V. & Sheetz, M. P. Cell fate regulation by coupling mechanical cycles to biochemical signaling pathways. *Curr. Opin. Cell Biol.* **21**, 38–46 (2009).
- Engler, A. J., Sen, S., Sweeney, H. L. & Discher, D. E. Matrix Elasticity Directs Stem Cell Lineage Specification. *Cell* **126**, 677–689 (2006).
- Chen, T. Y., Erickson, M. J., Crowell, P. A. & Leighton, C. Surface Roughness Dominated Pinning Mechanism of Magnetic Vortices in Soft Ferromagnetic Films. *Phys. Rev. Lett.* **109**, 097202–097206 (2012).
- Li, Z. B., Shen, B. G., Niu, E. & Sun, J. R. Nucleation of reversed domain and pinning effect on domain wall motion in nanocomposite magnets. *Appl. Phys. Lett.* **103**, 062405–062408 (2013).
- Rezende, S. M. & Azevedo, A. Dipolar narrowing of ferromagnetic resonance lines. *Phys. Rev. B* **44**, 7062–7065 (1991).
- Love, J. C., Urbach, A. R., Prentiss, M. G. & Whitesides, G. M. Three-Dimensional Self-Assembly of Metallic Rods with Submicron Diameters Using Magnetic Interactions. *J. Am. Chem. Soc.* **125**, 12696–12697 (2003).
- Sun, J. F., Sui, Y., Wang, C. & Gu, N. The investigation of frequency response for the magnetic nanoparticle assembly induced by time-varied magnetic field. *Nanoscale Res. Lett.* **6**, 453–458 (2011).
- Kang, K. S. *et al.* Regulation of osteogenic differentiation of human adipose-derived stem cells by controlling electromagnetic field conditions. *Exp. Mol. Med.* **45**, e6–e14 (2013).
- Chang, K.-A. *et al.* Biphasic Electrical Currents Stimulation Promotes both Proliferation and Differentiation of Fetal Neural Stem Cells. *PLoS ONE* **6**, e18738–e18748 (2011).
- Schäfer, R. Functional investigations on human mesenchymal stem cells exposed to magnetic fields and labeled with clinically approved iron nanoparticles. *BMC Cell Biol.* **11**, 22–38 (2010).
- Liu, X. *et al.* Oxytocin deficiency impairs maternal skeletal remodelling. *Biochem. Biophys. Res. Commun.* **388**, 161–166 (2009).

## Acknowledgments

This work is supported by grants from National Basic Research Program of China (2011CB933503, 2013CB733801) and National Natural Science Foundation of China (NSFC, 21273002, 81100625). J. F. Sun is also thankful to supports from National Natural Science Foundation of Jiangsu Province (BK2011590), 'QingLan' project of Jiangsu province, special fund for the top doctoral thesis of Chinese Education Ministry (201174) and the Fundamental Research Funds for the Central Universities (Southeast grant for young faculty). Yana Guan, Jie Zhang and Dr. Shijun Yuan are greatly appreciated for helpful discussion.

## Author contributions

J.S. conceived the project and wrote manuscript. J.S. and N.G. designed the experiments. J.S. and H.L. did the assembly of magnetic nanoparticles and the characterization. L.S. and Y.Z. synthesized the  $\gamma$ -Fe<sub>2</sub>O<sub>3</sub> nanoparticles. X.L. and Z.C. carried out the animal experiments, the cell culturing and the measurements. J.S. and N.G. manufactured the magnetic field generator. Y.L. gave some instructions on cell culturing and sterilization. J.H. did the experiments on cytoskeleton, western blotting. All authors reviewed the manuscript.

## Additional information

Supplementary information accompanies this paper at <http://www.nature.com/scientificreports>

**Competing financial interests:** The authors declare no competing financial interests.

**How to cite this article:** Sun, J. *et al.* Magnetic assembly-mediated enhancement of differentiation of mouse bone marrow cells cultured on magnetic colloidal assemblies. *Sci. Rep.* **4**, 5125; DOI:10.1038/srep05125 (2014).



This work is licensed under a Creative Commons Attribution-NonCommercial-NoDerivs 3.0 Unported License. The images in this article are included in the article's Creative Commons license, unless indicated otherwise in the image credit; if the image is not included under the Creative Commons license, users will need to obtain permission from the license holder in order to reproduce the image. To view a copy of this license, visit <http://creativecommons.org/licenses/by-nc-nd/3.0/>